Design and Optimization of Sensing-Communication Integration System in Industrial Automation based on FDA and PA

Freddy Y.P. Feng*, De Mi†, Mingxiang Guan*, Lichao Sun‡, Hui Tang*, Chang Liu§, Pei Xiao¶ and Chen Lu*
* Shenzhen Institute of Information Technology, Shenzhen, China
† College of Computing, Birmingham City University, Birmingham, United Kingdom
‡ School of Engineering, Lancaster University, Lancaster, United Kingdom
§ Extend Robotics Limited, Reading, United Kingdom
¶ Institute for Communication Systems, University of Surrey, Guildford, United Kingdom
Email: freddy.yp.feng@gmail.com, de.mi@bcu.ac.uk, gmx2020@126.com, l.sun9@lancaster.ac.uk,
tangh@sziit.edu.cn, chang.liu@extendrobotics.com, p.xiao@surrey.ac.uk, luchen@sziit.edu.cn

***Abstract*—Industrial automation is a rapidly evolving field that aims to improve efficiency, productivity, and safety in various verticals. The integration of sensing and communication technologies has become crucial in this automation process. Recent advancements in Frequency Diverse Array (FDA) antennas have shown promising performance advantages over traditional phased array antennas in certain aspects, e.g., the FDA-based radar can focus its beam in both angle and range domains simultaneously. In this paper, we propose a novel architecture for sensing-communication integration in the context of industrial automation, where FDA antennas are employed as the radar sensing array, while phased array antennas are utilized for communication purposes. The integration of FDA antennas brings benefits such as more accurate object detection, improved spatial resolution, and efficient data transmission. We present a comprehensive analysis of the proposed architecture, including design considerations, system modeling, and performance evaluation. The results demonstrate the potential of FDA antennas in enhancing the sensing-communication integration in industrial automation, leading to improved efficiency, productivity, and safety in industrial environments.**

I. Introduction

Industrial automation is a rapidly evolving field that aims to improve efficiency, productivity, and safety in various industries. The integration of sensing and communication plays a pivotal role in this automation process. In particular, the need for a seamless integration of sensing and communication capabilities has led to the development of the concept of sensing-communication integration [1]–[4].

Traditional phased array antennas have been widely used in industrial automation for both sensing and communication purposes. However, recent advancements in Frequency Diverse Array (FDA) antennas have shown promising performance advantages over traditional phased array antennas in certain aspects [7]–[9]. FDA antennas offer enhanced capabilities in terms of distance-angle correlation and three-dimensional beamforming, making them a promising solution for radar sensing applications [10]–[12].

In this paper, we propose a novel architecture for sensing communication integration in industrial automation, where FDA antennas are employed as the radar sensing array, while phased array (PA) antennas are utilized for communication purposes. By leveraging the superior performance of FDA antennas in radar sensing, we aim to enhance the overall system performance in terms of detection accuracy, range resolution, and robustness to interference.

The integration of FDA antennas in the sensing-communication architecture brings several benefits. Firstly, the distance-angle correlation feature of FDA antennas enables more accurate and reliable detection of objects in the industrial environment. This is particularly important for applications such as object tracking, collision avoidance, and environmental monitoring. Secondly, the three-dimensional beamforming capability of FDA antennas allows for improved spatial resolution and localization accuracy. This is crucial for precise positioning and tracking of objects in industrial automation scenarios. Lastly, by utilizing phased array antennas, we can ensure efficient and reliable data transmission between different components of the industrial automation system. The use of phased array antennas enables beamforming and beam steering capabilities, which enhance the signal quality, coverage, and capacity of the communication links.

In this paper, we present a comprehensive analysis of the proposed sensing-communication integration architecture, including the design considerations, system modeling, and performance evaluation. The convergence of FDA radar with PA-based communication subsystems has given rise to a novel RadComm system. The optimization challenges within the realm of RadComm are multifaceted. Traditional optimization problems in RadComm typically prioritize the performance of either communication or radar systems, often employing a rigid threshold to constrain the other. However, improper threshold settings can render these problems unsolvable, which calls for a more robust approach [5], [6], [20]. We adopt a bilevel programming framework to tackle these issues. It is

important to acknowledge the inherent complexity of bilevel programming, which is known to be strongly NP-hard, even in its simplest form, making it challenging to find polynomial algorithms that guarantee global optimality [13], [14].

Contributions: We introduce a novel transmitter design for an integrated RadComm system, leveraging both PA and FDA techniques to cater for communication and radar functions, respectively. The design includes a novel hybrid PA and FDA precoding scheme. We formulate the optimization problems with the aim of maximizing achievable sum-rates and minimizing Mean Square Error (MSE). These optimization problems adhere to given constraints related to FDA-based radar performance and total system power budget; We conduct experiments to validate the effectiveness of the FDA radar sensing array and phased array communication system in improving the overall performance of the industrial automation process. The results of our study demonstrate the potential of FDA antennas in enhancing the sensing-communication integration in industrial automation. The proposed architecture offers improved detection accuracy, range resolution, and communication reliability, leading to enhanced efficiency, productivity, and safety in industrial environments.

II. System Model

This section commences by elucidating the design and construction of the transmitter unit employing the hybrid approach of PA and FDA for RadComm applications. Subsequently, it delves into a comprehensive exploration of the system's architecture, channel model, and the intricacies of received signals, encompassing both radar signals and communication data streams.

A. Transmitter of PA-based Communications

First, we introduce the communication structure. Assume the integrated RadComm base station (BS) is equipped with N antennas serves M mobile stations (MSs), where each MS has N_{ms} antennas. For the communication part of RadComm, we assume that each MS needs to receive one data stream, e.g. the signal that the m-th user receives is $s_m(t), m = 1, 2, \cdots, M$, and this signal is precoded by the m-th column $\mathbf{u}_m \in \mathbb{C}^N$ of the communication precoding matrix $\mathbf{U} \in \mathbb{C}^{N\times M}$. This is the same as conventional communication precoding.

However, to accommodate the FDA radar mechanism, we propose an innovative signal modulation scheme. We add different frequency offsets to each precoded signal, e.g. the frequency offset for the m-th precoded signal is Δf_m. Then, we combine all these M signals and modulate them to the carrier frequency f_0 suitable for transmission, and transmit all the signals to the wireless channel.

From above, it can be seen that the actually transmitted frequency of the m-th signal is $f_m = f_0 + \Delta f_m, m = 1, 2, \cdots, M$.

B. Transmitter of FDA-based Radar

To proceed, we contemplate a mono-static radar system where the transmitting and receiving radar systems share an antenna array with the communication BS. To incorporate the FDA precoding into the existing communication PA precoding, we disperse the elements of the FDA precoding vector $\mathbf{t}$ into different columns of the PA precoder $\mathbf{U}$, achieving simultaneous precoding of signals for both PA and FDA. The specific procedure, involves constructing a zeros matrix $\mathbf{E} \in \mathbb{R}^{N\times M}$ of the same size as $\mathbf{U}$. Subsequently, we determine the positions to insert the elements of the FDA precoding vector $\mathbf{t}$, marking these positions with 1 and the rest with 0.

After that, the elements of $\mathbf{t}$ are filled row by row into the non-zero positions of matrix $\mathbf{E}$. It should be noted that the frequency offsets of each column of matrix $\mathbf{E}$ are the same as those of the corresponding column of $\mathbf{U}$. Then, by combining each column of $\mathbf{E}$, modulating to the carrier frequency f_0, the FDA signal is transmitted over the wireless channel. At this time, the frequencies of the electromagnetic waves radiated by each antenna are not identical, which is also a characteristic of FDA radars.

For the mechanism of setting the non-zero element positions of $\mathbf{E}$, the following rules can be followed. We first need to determine the frequency offsets of the electromagnetic waves to be transmitted by different antennas, which will be discussed later in the paper. Then, assuming it is determined that the n-th antenna transmits the signal with the m-th frequency offset, the element $\mathbf{E}(n, m)$ needs to be set to 1.

It should be noted that this matrix structure has to meet the following two rules:

1) Each row of $\mathbf{E}$ should contain only one element with value 1, while all other elements are 0.
2) All the 1s should be filled into at least two columns of $\mathbf{E}$.

The FDA precoding distributed into $\mathbf{E}$ can be mathematically expressed as

$$\mathbf{V} = \text{diag}(\mathbf{t})\mathbf{E}. \tag{1}$$

Meanwhile, the final transmission frequencies of each antenna can also be mathematically expressed as

$$\mathbf{f} = \mathbf{E}\Delta\mathbf{f} + f_0, \tag{2}$$

where $\Delta\mathbf{f} = [\Delta f_1, \ \cdots, \ \Delta f_M]^T$.

C. Hybrid PA and FDA Transmitter

Now, we present the transmitter with hybrid PA and FDA precoding, as shown in Fig. 1.

The hybrid PA and FDA precoding matrix $\mathbf{W} \in \mathbb{C}^{N\times M}$ based on this transmitter, is the superposition of the original PA communication precoding matrix $\mathbf{U}$ and the FDA precoding matrix $\mathbf{V}$, which can be mathematically expressed as

$$\mathbf{W} = \mathbf{U} + \mathbf{V}. \tag{3}$$

Since the PA communication and FDA radar share the same radio source, the FDA radar signal can be expressed as :

$$\mathbf{s}_r = \mathbf{E}\mathbf{s}, \tag{4}$$

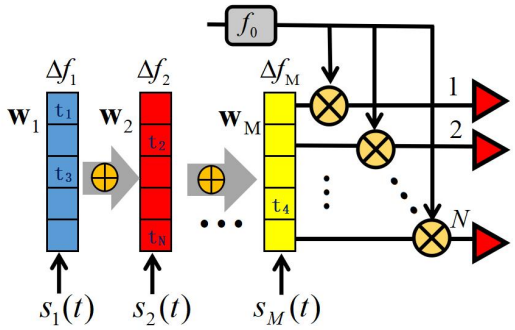

Fig. 1: Implementation procedure of hybrid PA and FDA transmitter.

where $\mathbf{s} = [s_1, s_2, \cdots, s_M]^T$ represents the input data streams. However, these data streams are time-varying signals. In order to obtain a constant radar signal, we let the radar beamformer $\mathbf{t}$ pre-absorb the radar signal $\mathbf{s}_r$, i.e., $\bar{\mathbf{t}} = \mathbf{t} \odot \mathbf{s}_r$, where $\odot$ denotes the Hadamard product that makes the input radar signal appear to be $\mathbf{1}_{M\times 1}$. For convenience, in the rest of this paper, we only consider the equivalent radar beamformer $\bar{\mathbf{t}}$, slightly abusing $\mathbf{t}$, which does not affect the final results.

D. Channel Model

In the considered scenario of multi-user MIMO, suppose that there are K_m scattering clusters between the m-th MS and the BS, and the radar target is located at (θ_0, r_0) with respect to the BS, where θ_0 is the direction of arrival (DoA), and r_0 is the distance between the target to the BS.

We assume that the k-th cluster between the m-th MS and the BS is located at $(\theta_{m,k}, r_{m,k})$ from the perspective of the BS, and at $(\phi_{m,k}, d_{m,k})$ from the perspective of the m-th MS. Here, $\theta_{m,k}$ and $\phi_{m,k}$ represent the direction of arrival (DoA) and angle of arrival (AoA) at the BS and m-th MS for the k-th cluster, respectively. Meanwhile, $r_{m,k}$ and $d_{m,k}$ denote the distances from the k-th cluster to the BS and m-th MS, respectively.

In our work, we model the communication channels based on the geometric MIMO channel model [15], [16], which can be readily extended to classical models such as Rayleigh and Rician channels. Since $\Delta f_m \ll f_0$, the attenuation coefficients of scattering clusters corresponding to different sub-carriers can be regarded as identical. Consequently, the channel between the BS and m-th MS can be formulated as

$$\mathbf{H}_m = \sum_{k=1}^{K_m} \alpha_{m,k} \mathbf{a}_{N_{\text{ms}}}(f_m, \phi_{m,k}, d_{m,k}) \mathbf{a}_N^H(f_m, \theta_{m,k}, r_{m,k}) \tag{5}$$

where $\alpha_{m,k}$ is the complex gain of the k-th cluster to the m-th MS and $\mathbf{a}_N(\cdot)$ denotes the PA steering vector with length N. When a uniform linear array (ULA) is assumed, the PA steering vector with length of N can be expressed as

$$\mathbf{a}_N(f_m, \theta, r) = \frac{1}{\sqrt{N}} [e^{j2\pi f_m \psi_1}, \ e^{j2\pi f_m \psi_2}, \cdots, \ e^{j2\pi f_m \psi_N}]^T, \tag{6}$$

where $\psi_n = (nd \sin\theta - r)/c_0$, and c_0 is the light velocity.

Similarly, we can express the monostatic FDA channel $\mathbf{G}$ from radar transmitter to the receiver through target as

$$\mathbf{G} = \alpha_0 \ \mathbf{g}(\mathbf{f}, \theta_0, r_0) \ \mathbf{g}^H(\mathbf{f}, \theta_0, r_0) \tag{7}$$

where α_0 denotes the radar cross section (RCS) of the target, and $\mathbf{g}(\mathbf{f}, \theta_0, r_0)$ is the FDA steering vector, which can be expressed as

$$\mathbf{g}(\mathbf{f}, \theta_0, r_0) = \frac{1}{\sqrt{N}} [e^{j2\pi f_1 \psi_1}, \ e^{j2\pi f_2 \psi_2}, \cdots, \ e^{j2\pi f_N \psi_N}]^T. \tag{8}$$

In reality, there exist numerous RadComm application scenarios, including vehicle radar with mobile phone communications, weather radar with WiFi communications, etc. Different scenarios exhibit distinct channel and interference characteristics. Therefore, it is imperative to constrain the analysis to a specific class of scenarios before delving into the RadComm problem. In this work, we presume the scenario satisfies the following operational constraints:

1) Compared to the distance between the target and radar, the communications between BS and MSs can be viewed as short-range. In other words, the distances between MSs and BS are much shorter than that between the target and radar/BS. Similarly, the scattering clusters are also much closer to the BS relative to the target-radar/BS separation.
2) Since $\Delta \mathbf{f} \ll f_0$, MSs are not equipped with accurate frequency filters to filter the sub-carriers of $\Delta \mathbf{f}$. However, the FDA-based radar receiver should have the capability to filter each sub-carrier, unlike communications.
3) In each period, there are no uplink signals from MSs to BS before the radar echo is received.

Based on these assumptions, we can proceed to analyze the received signals at both MSs and radar.

Now, we consider a more general case that each MS needs to receive S data stream at the same time, and correspondingly, the communications precoder for each MS need to extend from one column to S columns as well. Let $\mathbf{s}_m \in \mathbb{C}^S$ denote the intended data streams for the m-th MS with $\mathbb{E}(\mathbf{s}_m \mathbf{s}_m^H) = \mathbf{I}_S$, where $\mathbf{I}_S$ is the S-dimensional identity matrix, and $\mathbf{W}_m \in \mathbb{C}^{N\times S}$ is the corresponding precoder. Since the target is much farther than the MSs and clusters from the BS, with comparable transmitted power for both radar and communications, the echo signal power from the target will be much lower than the received signal power at MSs. Hence, the interference from target echoes can be ignored at the MSs.

Then, the received signal at the m-th MS can be expressed as:

$$\mathbf{y}_m = \underbrace{\mathbf{H}_m \mathbf{W}_m \mathbf{s}_m}_{\text{RadComm signals}} + \underbrace{\sum_{n\neq m}^{M} \mathbf{H}_m \mathbf{W}_n \mathbf{s}_n}_{\text{RadComm interference}} + \mathbf{n}_m, \tag{9}$$

and accordingly the SINR of the m-th MS signal is given by:

$$\text{SINR}_m = \text{Tr}(\mathbf{C}_m^{-1} \mathbf{W}_m^H \mathbf{H}_m^H \mathbf{H}_m \mathbf{W}_m) \tag{10}$$

where $\mathbf{n}_m$ is a vector of additive white Gaussian noise with zero-mean and its covariance matrix is given by $\mathbb{E}(\mathbf{n}_m\mathbf{n}_m^H) = \sigma_c^2\mathbf{I}_{N_{\text{ms}}}$, $\mathbf{C}_m = \mathbf{H}_m(\sum_{n\neq m}\mathbf{W}_n\mathbf{W}_n^H)\mathbf{H}_m^H + \sigma_c^2\mathbf{I}$.

III. Joint Optimization for PA and FDA Precoders

Consider a P2P MIMO communication system, where there is only one MS equipped with M antenna elements. The received signal at the MS is expressed as:

$$\mathbf{y} = \mathbf{HWs} + \mathbf{n}, \tag{11}$$

where $\mathbf{n}$ is a vector of additive white, zero-mean Gaussian noise with the covariance matrix of $\mathbb{E}(\mathbf{nn}^H) = \sigma^2\mathbf{I}_M$. In case we are dealing with multiple data-streams, the MS uses an equalizer in order to correctly detect each data stream. This can be mathematically expressed as:

$$\tilde{\mathbf{y}} = \mathbf{Q}^H\mathbf{HWs} + \mathbf{Q}^H\mathbf{n}, \tag{12}$$

where $\mathbf{Q}$ denotes the combiner/equalizer at the MS.

As mentioned previously, we aim to examine the robustness of the proposed joint PA and FDA scheme under various networks by taking different objectives in the both scenarios of MU-MISO and P2P MIMO. As for the P2P MIMO, we aim at minimizing the MSE at the MS side. Accordingly, the problem of optimizing the RadComm system in the P2P MIMO communication scenario can be formulated as:

$$\begin{cases} \min\limits_{\mathbf{t},\{\mathbf{u}_m\}_{1:M},\mathbf{Q}} & \mathbb{E}(||\mathbf{Q}^H\mathbf{HWs} + \mathbf{Q}^H\mathbf{n} - \mathbf{s}||^2) \\ \text{s.t.} & \mathbf{t} \in \{\arg\min\limits_{\mathbf{t}} \mathbf{t}^H\mathbf{R}_t\mathbf{t} : \mathbf{g}^H\mathbf{t} = \sqrt{p_t}\}, \\ & \sum\limits_{m=1}^{M} ||\mathbf{g}^H\mathbf{u}_m||^2 \leq \gamma, \\ & ||\mathbf{W}||^2 \leq P_0, \end{cases} \tag{13}$$

where $\mathbf{w}_m = \mathbf{u}_m + \mathbf{\Lambda_t e}_m$ and $\mathbf{W} = [\mathbf{w}_1, \mathbf{w}_2, \cdots, \mathbf{w}_M]$. Similarly, in the MU-MISO scenario, the optimization problem in (13), can also be divided into three sub-problems:

$$\begin{cases} \min\limits_{\{\mathbf{w}_m\}_{1:M},\mathbf{Q}} & \mathbb{E}(||\mathbf{Q}^H\mathbf{HWs} + \mathbf{Q}^H\mathbf{n} - \mathbf{s}||^2) \\ \text{s.t.} & ||\mathbf{W}||^2 \leq P_0 \end{cases} \tag{14a}$$

$$\begin{cases} \min\limits_{\mathbf{t}} & \mathbf{t}^H\mathbf{R}_t\mathbf{t} \\ \text{s.t.} & \mathbf{g}^H\mathbf{t} = \sqrt{p_t} \end{cases} \tag{14b}$$

$$\begin{cases} \min\limits_{\{\mathbf{u}_m\}_{1:M}} & \sum\limits_{m=1}^{M} ||\mathbf{u}_m + \mathbf{\Lambda_t e}_m - \mathbf{w}_m^o||^2 \\ \text{s.t.} & \sum\limits_{m=1}^{M} ||\mathbf{g}^H\mathbf{u}_m||^2 \leq \gamma \end{cases} \tag{14c}$$

To solve the optimization problem, we employ the alternating optimization method [18] to switch alternatively between constants and variables roles of namely $\mathbf{W}$ and $\mathbf{Q}$ until convergence. First, we fix $\mathbf{W}$ as constant and consider $\mathbf{Q}$ as the optimization variable, and then the problem turns into an unconstrained problem, which can be directly solved by equating its differentiation to zero and directly evaluate the optimum value $\mathbf{Q}^o$.

For convenience, we define the objective function as

$$\begin{aligned} f_0 &\triangleq \mathbb{E}(||\mathbf{Q}^H\mathbf{HWs} + \mathbf{Q}^H\mathbf{n} - \mathbf{s}||^2 \\ &= \text{Tr}(\mathbf{Q}^H\mathbf{HWW}^H\mathbf{H}^H\mathbf{Q} + \sigma^2\mathbf{Q}^H\mathbf{Q} - 2\mathbf{Q}^H\mathbf{HW} + \mathbf{I}_M). \end{aligned} \tag{15}$$

Differentiating f_0 with respect to $\mathbf{Q}$, yielding:

$$\frac{df_0}{d\mathbf{Q}} = 2(\mathbf{HWW}^H\mathbf{H}^H + \sigma^2\mathbf{I})\mathbf{Q} - 2\mathbf{HW}. \tag{16}$$

By equating the derivative with zero, the solution to this equation gives the optimal value of $\mathbf{Q}$ as:

$$\mathbf{Q}^o = (\mathbf{HWW}^H\mathbf{H}^H + \sigma^2\mathbf{I})^{-1}\mathbf{HW}. \tag{17}$$

Substituting $\mathbf{Q}$ with $\mathbf{Q}^o$ and dealing with the minimization equation and its KKT conditions, yield the optimal $\mathbf{W}$. The Lagrangian function with respect to $\mathbf{W}$ can be formulated as:

$$\begin{aligned} L(\mathbf{W}, \lambda_w) =& \text{Tr}(\mathbf{W}^H\mathbf{H}^H\mathbf{QQ}^H\mathbf{HW} - 2\mathbf{Q}^H\mathbf{HW}) \\ &+ \lambda_w(\text{Tr}(\mathbf{W}^H\mathbf{W}) - P_0). \end{aligned} \tag{18}$$

Differentiating the Lagrangian function with respect to $\mathbf{W}$, the optimal $\mathbf{W}$ can be evaluated as:

$$\mathbf{W}^o = (\mathbf{H}^H\mathbf{QQ}^H\mathbf{H} + \lambda_w\mathbf{I})^{-1}\mathbf{H}^H\mathbf{Q}, \tag{19}$$

which is a function of λ_w. According to complementary slackness [17], any optimal point $\mathbf{W}^o$ must satisfy the following equality constraint:

$$f_w(\lambda_w) = \text{Tr}((\mathbf{W}^o)^H\mathbf{W}^o) - P_0 = 0. \tag{20}$$

The differentiation of the function $f_w(\lambda_w)$, can be derived simply as:

$$f_w'(\lambda_w) = -2\text{Tr}(\mathbf{Q}^H\mathbf{H}(\mathbf{H}^H\mathbf{QQ}^H\mathbf{H} + \lambda_w\mathbf{I})^{-3}\mathbf{H}^H\mathbf{Q}). \tag{21}$$

Since $\mathbf{H}^H\mathbf{QQ}^H\mathbf{H} + \lambda_w\mathbf{I} \succ \mathbf{0}$, f_w is monotonically decreasing, the solution to the equation $f_w(\lambda_w) = 0$ can be obtained by applying the bisection or Newton method in the range $\mathbf{H}^H\mathbf{QQ}^H\mathbf{H} + \lambda_w\mathbf{I} \succ \mathbf{0}$.

By substituting λ_w^o into (19), we can obtain the optimal value $\mathbf{W}^o$. With $\mathbf{t}^o$ and $\mathbf{W}^o$, by solving (14c), we can obtain the optimal value of $\{\mathbf{u}_m^o\}_{1:M}$. Then, the final precoder can be expressed as:

$$\mathbf{w}_m^* = \mathbf{u}_m^o + \mathbf{\Lambda}_{\mathbf{t}^o}\mathbf{e}_m,\ m = 1, 2, \cdots, M, \tag{22}$$

where $\mathbf{\Lambda}_{\mathbf{t}^o} = \text{diag}(\mathbf{t}^o)$.

IV. Numerical Analysis

In this section, we consider an MU-MISO and a P2P MIMO wireless network with an FDA-based radar system, respectively. If not otherwise specified, we assume the BS/radar is equipped with $N = 64$ antenna elements, the RF frequency is $f_0 = 10$ GHz, the target is located at $(0°, 25$ km) and the noise power of each MS is the same as $\sigma_{c,m}^2 = \sigma^2 = 1, m = 1, 2, \cdots, M$. Each of the M subcarrier frequencies is assigned with $f_{\text{rnd}} \cdot 50$ kHz, where f_{rnd} is a normal Gaussian random variable, i.e., $f_{\text{rnd}} \sim \mathcal{N}(0, 1)$. As for the FDA-based radar, we set the desired waveform covariance matrix as $\mathbf{R}_t = \mathbf{I}$, $p_t = 10$ and the threshold of interference power is $\gamma = 0.1$.

A. P2P MIMO System

Now, we consider a downlink P2P MIMO communications system, in which there is only one MS equipped with $M = 5$ antenna elements serving the same number, $M = 5$, of data streams. As presented in Sec. III, for P2P MIMO system, we have considered the objective of joint PA and FDA precoder as minimizing its MSE. Similarly, in order to eliminate the impacts of power budget, we considered the normalized MSE with respect to P_0, which can be expressed as:

$$\overline{\text{MSE}} = \mathbb{E}(||\mathbf{Q}^H\mathbf{H}\mathbf{W}\mathbf{s} + \mathbf{Q}^H\mathbf{n} - \mathbf{s}||^2)/P_0. \quad (23)$$

For convenience, we refer to the optimal precoder $\mathbf{W}^o$ in (19) as "OptAlg in only communication system", which can be considered as a reference baseline precoder, and denote the final precoder $\mathbf{W}^*$ solved by (22) as "OptAlg in RadComm system". Additionally, to evaluate the proposed scheme, we also compared it with other final precoders that based on conventional P2P precoders, such as singular value decomposition (SVD), MRC, MMSE. As we have done with the case of MU-MISO scenario, we study the impact of total power budget, P_0, as well as the radar transmit power, p_t, constraints on the communication performance. We first vary the value of P_0/σ^2 from 0 dB to 30 dB, while keeping $p_t = 10$.

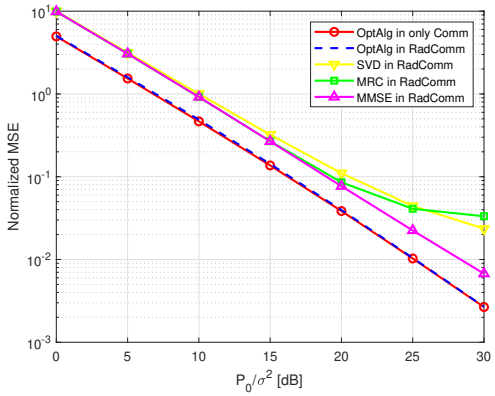

Fig. 2: Normalized MSE Vs. power budget in P2P MIMO scenarios.

It is obvious from Fig. 2 and Fig. 3, as P_0 increases, the normalized MSE and the spectrum efficiency with all the percoders have improved at a fast rate. Additionally, the approach named "OptAlg in only communications" can be considered as lower bound for the normalized MSE and an upper bound for the spectrum efficiency. Although the approach named "OptAlg in RadComm" can not achieve such lower and upper bounds, it provides the best performance in terms of normalized MSE and spectrum efficiency among all legacy precoding algorithms, such as applying SVD, MRC, and MMSE precoders in RadComm system.

While keeping p_t as a constant, fixed radar power, as the total power increases, additional power has to be allocated to communications, which improves the system performance in terms of either normalized MSE or spectrum efficiency as the

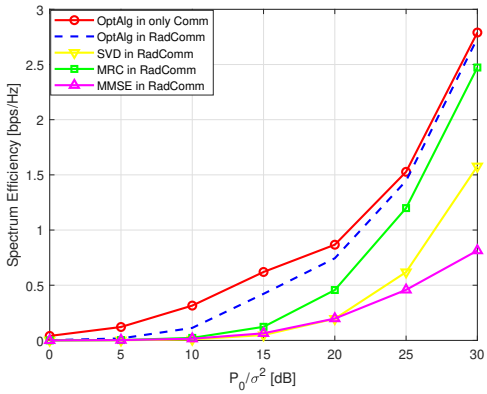

Fig. 3: Spectrum efficiency Vs. power budget in P2P MIMO scenarios.

optimization objective. Moreover, since the approach named "OptAlg in only communications" is optimal in terms of minimizing MSEs, it is thus expected that the approach named OptAlg provides the optimal performance with normalized MSE. The precoder of "OptAlg in RadComm" can also achieve almost the same performance with the precoder of "OptAlg in only communications", which shows that the proposed scheme can robustly achieve the optimal performance in terms of normalized MSE. For other precoders including MRC, SVD and MMSE, despite their simplicity, they suffer significant performance loss in terms of both normalized MSE and spectrum efficiency. From the above discussion, it can be concluded that the proposed OptAlg can be considered as the optimal solution in both the MSE and spectrum efficiency-based optimization scenarios.

Finally, we discuss the impact of the radar transmit power p_t on the communications performance. The radar transmit power, p_t, takes values in the range from 0 to 100, while keeping P_0/σ^2 as constant equals 30 dB.

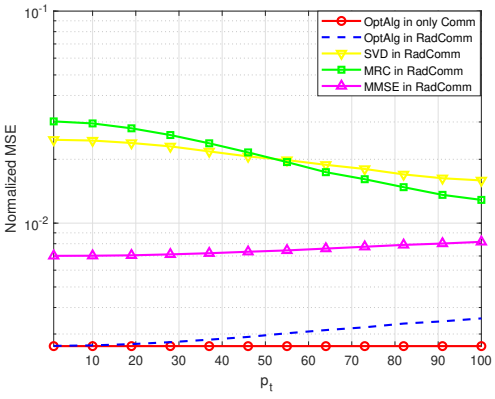

Fig. 4: Normalized MSE Vs. p_t in P2P MIMO scenario.

It can be seen from Fig. 4 and Fig. 5 that the communication performance slightly degrades as the radar transmit power p_t increases, i.e., spectrum efficiency decreases and parts of

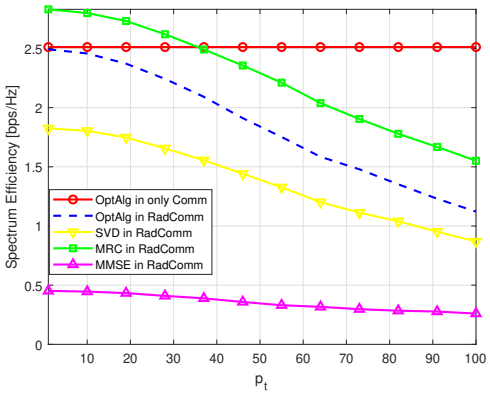

Fig. 5: Spectrum efficiency Vs. p_t in P2P MIMO scenario.

normalized MSE increases. Additionally, we also note that the normalized MSE varies slowly as p_t increases according to the precoding approach. Although OptAlg algorithm still works well in terms of both normalized MSE and spectrum efficiency, while the performance of MRC and SVD is the worst. Since all the sensing or detection parameters of the radar system depend mainly on p_t, when p_t increases, this means that more power has to be allocated to the radar, thus less power is left for serving communication tasks, which in turn results in poor communication performance.

When using minimizing MSE as the objective of optimization, the proposed OptAlg shows the best performance in terms of normalized MSE, however, in this case we have not target the spectrum efficiency in any sense, which in turn can not guarantee the performance in terms of the spectrum efficiency. But, the numerical results show that OptAlg produces an excellent performance in terms of the spectrum efficiency, especially at high levels of p_t. From the above discussion, we can conclude that the proposed algorithm, OptAlg, can be considered the best candidate method for designing joint PA and FDA precoder in the RadComm system.

V. Conclusion

The integration of sensing and communication technologies in industrial automation is crucial for improving efficiency, productivity, and safety. Recent advancements in FDA antennas have shown promising performance advantages over traditional phased array antennas in certain aspects. By employing FDA antennas as the radar sensing array and phased array antennas for communication purposes, we have proposed a novel architecture for sensing-communication integration in industrial automation. The integration of FDA antennas brings benefits such as more accurate object detection, improved spatial resolution, and efficient data transmission. Through comprehensive analysis and performance evaluation, we have demonstrated the potential of FDA antennas in enhancing the overall system performance. The proposed architecture offers improved efficiency, productivity, and safety in industrial environments, making it promising candidate for future industrial automation applications.

Acknowledgment

This work is support by Shenzhen Municipal Commission of Science and Technology Innovation with the grant funding numbers of 20220818232202001 and GJHZ20220913143013024.

References

[1] S. H. Dokhanchi, M. R. B. Shankar, Y. A. Nijsure, T. Stifter, S. Sedighi and B. Ottersten, "Joint automotive radar-communications waveform design," 2017 IEEE PIMRC, Montreal, QC, Canada, 2017, pp. 1-7.

[2] K. Han and S. Hong, "Detection and Localization of Multiple Humans Based on Curve Length of I/Q Signal Trajectory Using MIMO FMCW Radar," in IEEE Microwave and Wireless Components Letters, vol. 31, no. 4, pp. 413-416, April 2021.

[3] K. Han and S. Hong, "Phase-Extraction Method With Multiple Frequencies of FMCW Radar for Human Body Motion Tracking," in IEEE Microwave and Wireless Components Letters, vol. 30, no. 9, pp. 927-930, Sept. 2020.

[4] W. Chung, C. -Y. Kim, S. S. Kim and S. Hong, "Design of 94-GHz Highly Efficient Frequency Octupler Using 47-GHz Current-Reusing Class-C Frequency Quadrupler," in IEEE Transactions on Microwave Theory and Techniques, vol. 68, no. 2, pp. 775-784, Feb. 2020.

[5] A. Hassanien, M. G. Amin, Y. D. Zhang and F. Ahmad, "A dual function radar-communications system using sidelobe control and waveform diversity," *2015 IEEE radar Conference (radarCon), Arlington*, VA, 2015, pp. 1260-1263.

[6] Liu, Fan, et al. "MU-MIMO communications with MIMO radar: From co-existence to joint transmission," *IEEE Transactions on Wireless Communications*, 2018, 17(4): 2755-2770.

[7] W. Q. Wang. "Frequency diverse array antenna: new opportunities," *IEEE Antennas and Propagation Magazine*, 2015, 57(2): 145-152.

[8] J. Xu, G. Liao, S. Zhu, et al. "Deceptive jamming suppression with frequency diverse MIMO radar," *Signal Processing*, 2015, 113: 9-17.

[9] J. Xiong, W. Wang, H. Shao and H. Chen, "Frequency Diverse Array Transmit Beampattern Optimization With Genetic Algorithm," in *IEEE Antennas and Wireless Propagation Letters*, vol. 16, pp. 469-472, 2017.

[10] W. Wang, "Retrodirective Frequency Diverse Array Focusing for Wireless Information and Power Transfer," in *IEEE Journal on Selected Areas in Communications*, 2019, 37(1), pp: 61-73.

[11] R. Gui, W. Wang, C. Cui and H. C. So, "Coherent Pulsed-FDA-based radar Receiver Design With Time-Variance Consideration: SINR and CRB Analysis," in *IEEE Transactions on Signal Processing*, vol. 66, no. 1, pp. 200-214, 1 Jan.1, 2018.

[12] Qin, Si, "Coprime Signal Processing for Spatial and Temporal Spectrum Sensing," *Villanova University*, 2016, pp: 108-129.

[13] P. Hansen, B. Jaumard, and G. Savard, "New branch-and-bound rules for linear bilevel programming," *SIAM Journal on Scientific and Statistical Computing*, 13:1194–1217, 1992.

[14] A. Sinha, P. Malo and K. Deb, "A Review on Bilevel Optimization: From Classical to Evolutionary Approaches and Applications," in *IEEE Transactions on Evolutionary Computation*, vol. 22, no. 2, pp. 276-295, April 2018.

[15] Q. H. Spencer, B. D. Jeffs, M. A. Jensen and A. L. Swindlehurst, "Modeling the statistical time and angle of arrival characteristics of an indoor multipath channel," in *IEEE Journal on Selected Areas in Communications*, vol. 18, no. 3, pp. 347-360, March 2000.

[16] E. Ben-Dor, T. S. Rappaport, Y. Qiao and S. J. Lauffenburger, "Millimeter-Wave 60 GHz Outdoor and Vehicle AOA Propagation Measurements Using a Broadband Channel Sounder," *2011 IEEE Global Telecommunications Conference - GLOBECOM 2011*, Houston, TX, USA, 2011, pp. 1-6.

[17] Park, Jaehyun, and Stephen Boyd. "General heuristics for nonconvex quadratically constrained quadratic programming," *arXiv preprint arXiv*:1703.07870 (2017).

[18] Goldstein, Tom, Brendan O'Donoghue, Simon Setzer, and Richard Baraniuk. "Fast alternating direction optimization methods," *SIAM Journal on Imaging Sciences*, no. 3 (2014): 1588-1623.

[19] Boyd, Stephen, Stephen P. Boyd, and Lieven Vandenberghe, "Convex optimization," *Cambridge university press*, 2004, pp: 243-244.

[20] F. Liu, C. Masouros, A. Li and T. Ratnarajah, "Robust MIMO Beamforming for Cellular and Radar Coexistence," in *IEEE Wireless Communications Letters*, vol. 6, no. 3, pp. 374-377, June 2017.